3x3 Dipole lens antenna at 300 GHz with different permittivity lenses

1st Mikko Kokkonen
Microelectronics research unit
University of Oulu
Oulu, Finland
Mikko.Kokkonen@oulu.fi

2nd Sami Myllymäki
Microelectronics research unit
University of Oulu
Oulu, Finland
Sami.Myllymaki@oulu.fi

3rd Heli Jantunen
Microelectronics research unit
University of Oulu
Oulu, Finland
Heli.Jantunen@oulu.fi

***Abstract*—In telecommunications (5G/6G) lenses can be used to manipulate the electric field emitted by an antenna. In this paper different permittivity lenses were studied with 3x3 dipole array acting as antenna source. Iterative study to the lens eccentricity showed different lenses for different permittivity where a low permittivity lens with heavily eccentric shape increased antenna gain by 14.6 dB and high permittivity lens gain by 9.9 dB and the total gain was 32 dB for low permittivity lens and 27 dB for higher permittivity lenses. With high permittivity lenses the whole lens surface was not illuminated by the feeding antenna.**

***Index Terms*—5G, 6G, Far field patterns, Lens antennas, Millimeter wave propagation, Near field patterns**

I. Introduction

In telecommunications frequency is climbing to the sub teraherz and interest to lenses with 5G/6G applications have grown significantly. Lenses came in varied sizes and shapes with lenses radiation pattern generated by an antenna can be manipulated. Lenses can turn the propagated field either a plane wave or focus it to a spot. Due the path loss high gain antenna needs to have 25-40 dBi in gain. [1]. The research question is how lens material should be selected and adjusted for the purpose of the lens. Currently available material options are silicon ($\varepsilon_r 11.5$) [2]–[4] and polymers ($\varepsilon_r 2.3$) [5]–[10]. In this paper three different half spherical lenses which have a radius 15 mm and a permittivity 2, 5, and 11, the lenses' effect on the antenna gain at 300 GHz is investigated by simulations. Theoretical maximum directivity for 15 mm lens antenna is 40 dBi. The above mentioned permittivity were chosen because $\varepsilon_r 2$ is close to the plastics and $\varepsilon_r 11$ is near to the permittivity of the silicon and $\varepsilon_r 5$ is just between of the other two. The lens size as wavelengths are 42λ, 67λ and 99λ, respectively. The loss tangent was set to be 4E-4 for all materials. 3x3 dipole array with a reflector was chosen to present a focused antenna. The antenna array to lens size ratios were 28, 44 and 66. Study was conducted without any changes to the antenna or loss tangent as the interest lays in the permittivity change. In Section 2 is given brief introduction to theories related to the antenna and lens parameters. Section 3 simulation results are reported and discussed. Section 4 concludes this paper.

This work has been supported by Academy of Finland 6Genesis Flagship (grant no.318927)

II. Theory

Directivity is defined as the ratio of the radiation of intensity in a certain direction to the average radiation intensity [11], or

$$D(\theta, \phi) = \frac{U(\theta, \phi)}{U_{ave}} \tag{1}$$

Directivity can also be presented using ratio between effective area A_e and wavelength λ,

$$D = \frac{4\pi A_e}{\lambda^2} \tag{2}$$

For aperture antennas, effective apertures are approximately equal to physics apertures ($A_e \simeq A_p$).

Gain is directly related to the directivity. The maximum gain of an antenna is equal to its maximum directivity multiplied by radiation efficiency [11], or

$$G = e_r D \tag{3}$$

Focal length and focus spot

$$\frac{1}{F} = (n-1)\left[\frac{1}{R_1} - \frac{1}{R_2} + \frac{(n-1)d}{nR_1R_2}\right], \tag{4}$$

where F is the focus, n is the refractive index, using relative permittivity this changes to $\sqrt{\varepsilon_r}$ [12] and the radiuses of curvatures R1 and R2.

Different field regions: Field around the antenna is typically divided into three different regions where size of the antenna element (D) and wavelength λ determines the region distance from the antenna. Closest to the antenna is reactive field where E- and H- fields are are out of phase by $90°$. After the reactive field is radiating field (fresnell region) where E- and H- fields starts to align and then there is far field where E- and H- field are orthogonal to each other. Equations for different regions are given in TABLE I.

Table I
DIFFERENT FIELD REGIONS

Region	distance from antenna (r)
Reactive near field	0 to $0.62\sqrt{\frac{D^3}{\lambda}}$
Radiating near field	$0.62\sqrt{\frac{D^3}{\lambda}}$ to $\frac{2D^2}{\lambda}$
Far field	$\frac{2D^2}{\lambda}$ to inf

III. SIMULATIONS

Simulations were done with CST, simulation parameters are following: Transient solver, hexahedral mesh having precision $\lambda/10$ and simulation precision -40 dB. Simulation model is following 3x3 dipole array acting as a focused antenna having 17 dB gain. Half spherical lens (15 mm radius) was set at 0.25 mm from the antenna array and antenna array was located at the center of the lens. Behind the array (0.25 mm) was a rectangular metal reflector (the length of the side of the reflector was the same as the lens diameter). Iterative simulations were used to change the height of the lens by scaling the z-axis of the lens in 0.1 steps. Iterations were performed until the gain was no longer increased and began to decrease. Iterative simulation was done for all the different permittivity lenses starting from the half spherical shape. Lens shapes from the iterative simulations are presented in the Fig. 1. From the single lens, three unique lenses with different gains are the results; a low permittivity lens has 24.45 mm height and eccentricity 0.79, medium permittivity has 16.50 mm and 0.42 and high permittivity has 15.00 mm and 0. Antenna lens

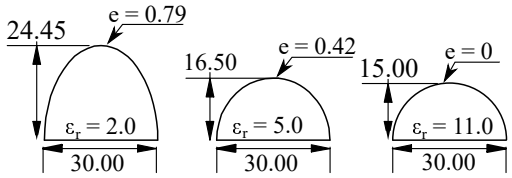

Figure 1. Result lenses from the simulation for different permittivities (ε_r), resulted shapes have different eccentricity (e). (Dimension units are in mm).

electrical properties are presented in Table II. With different eccentrics, lens antenna gains vary between 26.9-31.6 dB, the lens increased the antenna gain by 9.9-14.6 dB. Form the original (15 mm radius) shape eccentricity increase with $\varepsilon_r 2$ lens gain improves by 11.9 dB and $\varepsilon_r 5$ lens gain improves only 3.3 dB. $\varepsilon_r 11$ lens did not have any improvement in gain even when the lens was made flatter.

As the resulted shapes are eccentric lens focus spot is simulated rather than calculated from the equation 4. Simulation

Table II
ANTENNA PARAMETERS

ε_r	Gain (dB)	Direction	HPBW	FNBW	SLL (dB)
Antenna	17.0	0.0°	38.0°	88.0°	14.5
2.0	31.6	0.0°	3.0°	7.0°	14.3
5.0	27.2	0.0°	8.0°	12.0°	12.3
11.0	26.9	0.0°	4.0°	22.0°	19.4

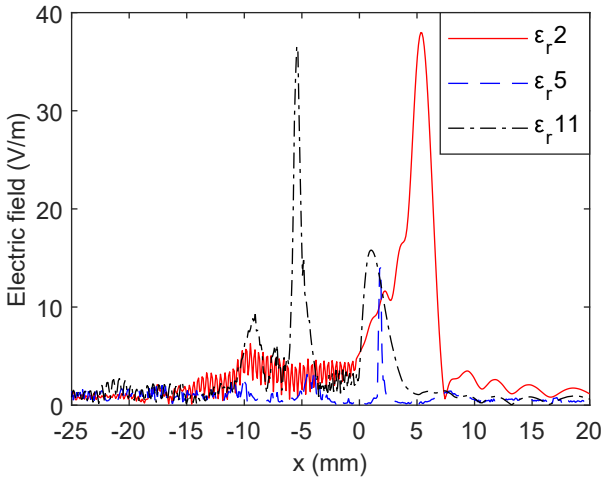

Figure 2. Simulated plane wave propagation with different lenses. The Plane wave was excited from -25 mm and the lens flat surface is at 0 mm and focal spots are located at the peaks' maximum on the positive side of the x-axis.

was conducted using a plane wave to illuminate the lens and line plot of the resulting 2D-electric field was plotted. The plotted result shows a line from the dead center of the lens spanning from the entire simulated length Fig2. Calculated focal lengths are following: 15 mm, 3.75 mm, and 1.5 mm ($\varepsilon_r 2$, $\varepsilon_r 5$, and $\varepsilon_r 11$). As the lenses' have the different radius of curvatures their focal lengths differ. Form the Fig.2, focal lengths locations are following: 5.4 mm, 1.9 mm, and 1.1 mm. None of the focal lengths are the same length and do not even match the antenna's distance from the lens (antenna array was at 0.25 mm from the lens). Electric field values at the peaks are following 37 V/m and 14-15 V/m where the excited plane wave had strength 1 V/m. The $\varepsilon_r 11$ lens has a visible electric field peak inside the lens (-5 mm) that indicates a resonance point. E-field 2-dimensional pictures are presented in Fig. 3. Near by lens E-field pattern are shown that antenna main lobes are gradually pushed towards the main lobe as the permittivity is increased. The lens surface is not well illuminated within the high permittivity material lenses, and almost the same beam characteristics might be achievable with a lower diameter lens. Almost the same directivity for silicon lenses can be achieved by 10 mm diameter lens presented in [2]–[4]. Low permittivity lens gain results are consistent with [8]–[10].

Part of the main beam investigated in line plot Fig4. In the plot electric field values from the 2D electric field plot are taken and presented as a line going through the dead center of the lens. In the plot is clear that electric field from the antenna array has the highest value at the antennas location and starts gradually dropping. The lenses with different permittivity have a different electric field intensity inside the lens and exited electric field intensity differs (also frequency have effect on the electric field behavior inside the lens and to the exited electric field [13]). Those intensity peaks inside the lens can be explained by the standing wave resonance that increases with the permittivity as the reflection intensity from the lens

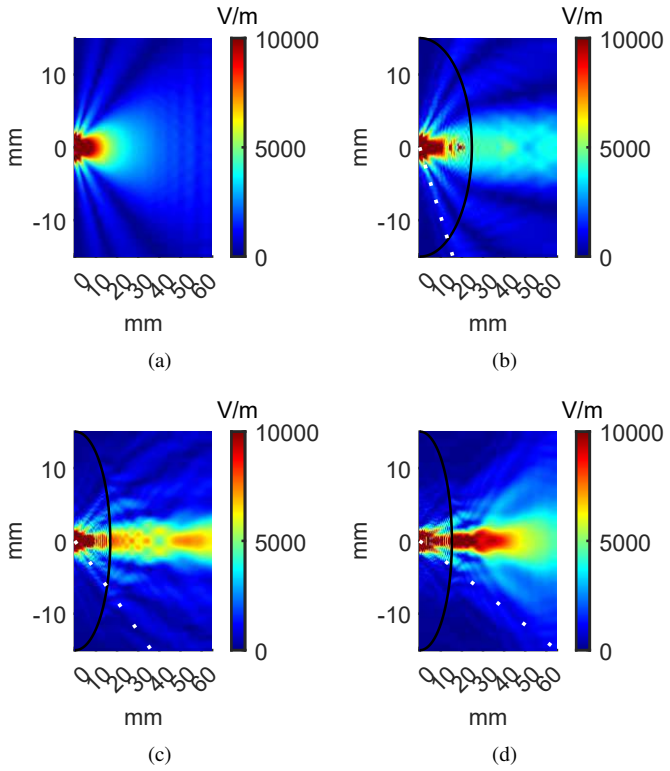

Figure 3. Simulation results of near fields a) antenna b) $\varepsilon_r 2.0$ c) $\varepsilon_r 5.0$ d) $\varepsilon_r 11.0$. Dotted line shows the approximate maximum angle of the near field.

surfaces increases and due to the case where a reflection matching layer is not used.

Phases of E- and H-field vectors were simulated in Fig. 5. The E- and H-field phases show far field characteristics close to 5 mm which is a lot closer than the calculated far field distance for 30 mm antenna (1800 mm Table I). The lens material is a passively behaving component for E- and H-fields, thus far field propagation is achieved before the wave

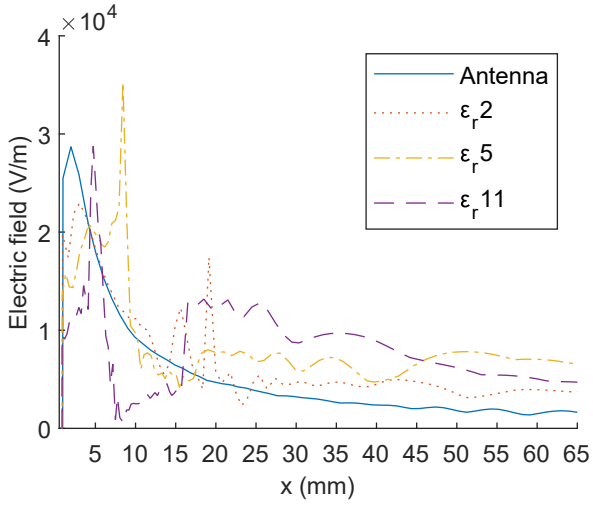

Figure 4. Simulated electric field change

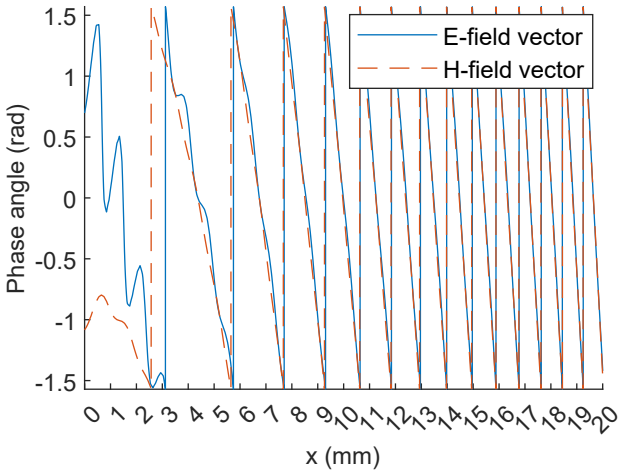

Figure 5. Simulated phase angle E- and H-field vectors of $\varepsilon_r 5$ lens

leaves the lens. Far field antenna patterns follow the near- by lens E-field patterns. Far field results are presented in Fig6. and antenna parameters in table II. Lens focuses the main lobe ie. collimate the beam which is seen as an increase in the lens antenna gain. As the antenna has half power beam width (HPBW) is 38 degrees and with lenses it shrinks by 30-35 degrees down to 3-6 degrees. Total radiation efficiency was -0.04 dB, -2.16 dB, -3.35 dB and -3.0 dB and radiation efficiency -1.41 dB -0.42 dB, -0.58 dB and -0.7 dB for the antenna and permittivity 2,5 and 11.

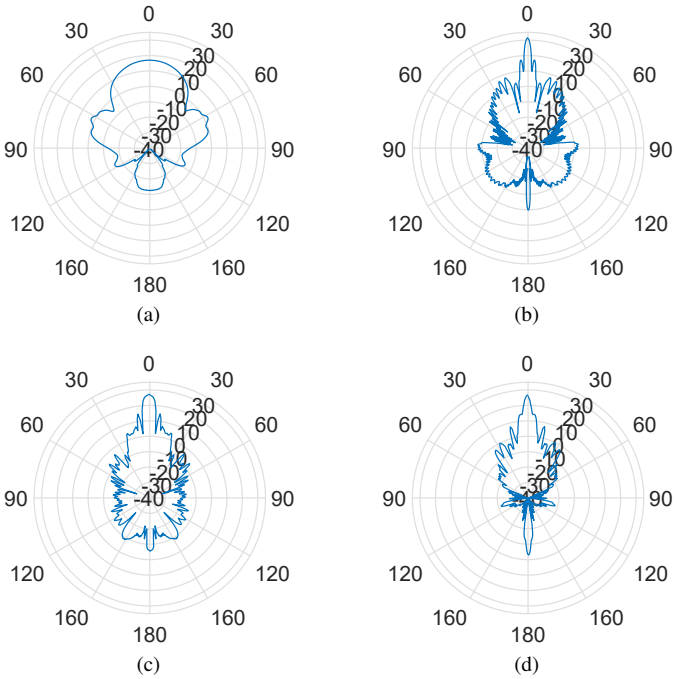

Figure 6. Simulation results of far fields a) antenna b) $\varepsilon_r 2.0$ c) $\varepsilon_r 5.0$ d) $\varepsilon_r 11.0$

IV. Conclusion

Table III has the comparison of different permittivity lenses and their impacts on different attributes. As the antenna and the loss tangent was kept the same then the results only show the effect to the lens shape and gain form the permittivity change. As its clear that lens made of low permittivity material tends to be more ellipsoidal (bullet shape) lens than lenses made of high permittivity material because lens focal distance needs to be close to the distance between the lens and the antenna. Inside the lens electric field strengths varies related to the permittivity and the field strength immediately after the lens varies as well. Phase behavior is not consistent with the different field region equations (Table I). The far field characteristics were achieved at 5 mm, way before the calculated distance 1.8 m. It is interesting to see the lens permittivity having an effect on the side lobe directions. As the permittivity increased side lobes tend to be pushed towards the main lobe. The high permittivity lens will give improvements to gain but the use of lower permittivity lens improvements to gain would be +4 dB more than the silicon-based lens. In the future low permittivity sustainable lenses will be studied.

Table III
Permittivity comparison

Attribute	**Small** ($\varepsilon_r 2$)	**Medium** ($\varepsilon_r 5$)	**High** ($\varepsilon_r 11$)
Eccentricity	Big	Low	None
Focus	Long (5.0 mm)	Small (1.5 mm)	Small (1.0 mm)
Near-field angle	Wide (15 mm)	Medium (35 mm)	Small (65 mm)
Main beam width	Narrow	Wide	Narrow
Directivity	Great	Medium	Medium

References

[1] T. Kürner, "THz Communications: Challenges and Applications beyond 100 Gbit/s," in *MWP 2018 - 2018 Int. Top. Meet. Microw. Photonics*, Tolouse, France, 2018.

[2] A. J. Alazemi, H. H. Yang, and G. M. Rebeiz, "Double Bow-Tie Slot Antennas for Wideband Millimeter-Wave and Terahertz Applications," *IEEE Trans. Terahertz Sci. Technol.*, vol. 6, no. 5, pp. 682–689, 2016.

[3] T. K. Nguyen and H. H. Tran, "Air gap effect on antenna characteristics of slitline and stripline dipoles on an extended hemispherical lens substrate," *Appl. Comput. Electromagn. Soc. J.*, vol. 33, no. 9, pp. 1018–1025, sep 2018.

[4] C. V. Vangerow, B. Goettel, H. J. Ng, D. Kissinger, and T. Zwick, "Circuit building blocks for efficient in-antenna power combining at 240 GHz with non-50 Ohm amplifier matching impedance," in *Dig. Pap. - IEEE Radio Freq. Integr. Circuits Symp.*, Honolulu, USA, 2017, pp. 320–323.

[5] R. Sauleau, C. A. Fernandes, and J. R. Costa, "Review of lens antenna design and technologies for mm-wave shaped-beam applications," in *ANTEM 2005 - 11th Int. Symp. Antenna Technol. Appl. Electromagn. Conf. Proc.*, St.Malo, France, 2005, pp. 1–5.

[6] E. Lacombe, F. Gianesello, H. Gulan, T. Zwick, C. Luxey, A. Bisognin, D. Titz, J. Costa, and C. A. Fernandes, "Low-cost 3D-printed 240 GHz plastic lens fed by integrated antenna in organic substrate targeting Sub-THz High data rate wireless links," *2017 IEEE Antennas Propag. Soc. Int. Symp. Proc.*, vol. 2017-Janua, pp. 5–6, 2017.

[7] J. Sun and F. Hu, "Three-dimensional printing technologies for terahertz applications: A review," *Int. J. RF Microw. Comput. Eng.*, vol. 30, no. 1, 2020.

[8] W. Pan and W. Zeng, "Far-field characteristics of the square grooved-dielectric lens antenna for the terahertz band," *Appl. Opt.*, vol. 55, no. 26, pp. 7330–7336, 2016. [Online]. Available: http://ao.osa.org/abstract.cfm?URI=ao-55-26-7330

[9] K. Konstantinidis, A. P. Feresidis, C. C. Constantinou, E. Hoare, M. Gashinova, M. J. Lancaster, and P. Gardner, "Low-THz Dielectric Lens Antenna with Integrated Waveguide Feed," *IEEE Trans. Terahertz Sci. Technol.*, vol. 7, no. 5, pp. 572–581, 2017.

[10] G. B. Wu, Y. S. Zeng, K. F. Chan, S. W. Qu, and C. H. Chan, "High-gain circularly polarized lens antenna for terahertz applications," *IEEE Antennas Wirel. Propag. Lett.*, vol. 18, no. 5, pp. 921–925, 2019.

[11] G. A. Stutzman, Warren L ; Thiele, *Antenna theory and design*, 2nd ed., G. A. Thiele, Ed. New York: Wiley, 1998.

[12] J. Kraus and R. Marhefka, *Antennas for all applications*, 3rd ed., B. A. Munk, Ed. Boston MA: McGraw-Hill, 2002, vol. 1, no. 34.

[13] M. Kokkonen, S. Myllymäki, and H. Jantunen, "Focal Length of a Low Permittivity Plano-Convex Lens at Frequencies 30-600 GHz," dec 2019. [Online]. Available: https://digital-library.theiet.org/content/journals/10.1049/el.2019.3158